Reflection from Irregular Array of Silver Nanoparticles on Multilayer Substrate

Victor Ovchinnikov
Department of Aalto Nanofab
School of Electrical Engineering, Aalto University
Espoo, Finland
e-mail: Victor.Ovchinnikov@aalto.fi

***Abstract*—Reflection from silver irregular arrays of nanostructures on quartz and oxidized silicon substrates is studied. It is shown that localized plasmon resonances in reflectance spectra cannot be easily identified by their peaks like it is done in case of extinction spectra. To clarify positions of resonances optical properties of samples are analyzed in relation to their design and morphology. Extinction and reflection from as prepared, plasma etched and SiO_2 covered samples are compared. It is concluded that coupling between nanoparticles, phase shift of scattered light and reflection from film interfaces lead to additional features in reflectance spectra in comparison with extinction ones. Recommendations for identification of plasmon resonances in reflectance spectra are proposed.**

Keywords-Ag nanoparticle; surface plasmon resonance; reflectance; extinction; irregular array.

I. INTRODUCTION

Plasmonic nanostructures are widely used in sensors, metamaterials, solar cells, photonics and spectroscopy [1]-[5]. Effective application of these structures is based on localized surface plasmon resonance (LSPR) demonstrated in ultraviolet, visible and infrared. The wavelength of LSPR depends on material and geometry of nanostructures, their interaction with each other and electromagnetic properties of environment, including substrate and capping layers. Despite on near field nature, LSPR can be observed in far field optical measurements due to variation in optical properties of the studied structures. Extinction is the most popular method of LSPR registration due to its simple implementation and straightforward interpretation, i.e., maximum and width of extinction peak correspond LSPR wavelength and damping, respectively. However, extinction can be measured only for non-opaque structures, e.g., for nanostructures on transparent substrates or for plasmonic colloidal particles. Furthermore, extinction spectra are not effective for overlapped peaks, when spectral deconvolution is not obvious.

LSPR on opaque substrates can be visualized by different kinds of reflection and scattering measurements. However, peak and trough of specular reflectance do not correspond to LSPRs and spectrum analysis becomes problematic. Scattering measurements require special arrangement of light illumination (dark field) to separate low scattering signal from strong reflection background. It limits range of measured samples by plasmonic nanostructures on substrate surface and, for example, plasmonic nanoparticles inside of dielectric matrix cannot be analyzed. In case of correlated scattering centers, i.e., when array of coupled nanostructures is analyzed, correspondence between scattered peaks and LSPRs is broken and LSPRs should be observed in specular reflectance. Additionally, scattering results are obtained in arbitrary units and cannot be used for comparison of different experiments. This happens, due to the problems with measurement of scattered reference spectrum for calibration procedure. In contrast, reflectance reference spectrum can be easily obtained for any material. Combination of total reflectance and diffuse reflectance is especially useful for analyzing plasmon structures, because the last one provides measurement of scattering in absolute values.

In this paper, we propose to use total reflectance for identification of LSPR on opaque and transparent substrates. It is demonstrated that wavelength position of LSPR correlates with peak and trough of reflectance in a clear way. Furthermore, overlapped peaks manifest themselves separately in reflectance spectra and can be easily distinguished.

This paper is organized in a following way. In the subsequent Section II, the details of sample preparation and the measurement procedures are presented. In Section III, the results of the work are demonstrated by scanning electron microscope (SEM) images as well as reflection and extinction spectra of the fabricated samples. The effect of the substrate and dielectric layers on reflectance of silver nanoparticles is discussed in Section III as well. In Section IV, the conclusions are drawn.

II. METHOD

Quartz or crystalline Si wafers (4” in diameter, 0.5-mm-thick) were used as substrates. The Al_2O_3 layer was grown on the substrate by atomic layer deposition (ALD), and SiO_2 layer was created by thermal oxidation of the Si wafer. Silver layers, with a thickness of 15 nm, were deposited by electron-beam evaporation with the deposition rate of 0.5 nm/s. Nanoparticle arrays were fabricated by ion beam mixing (IBM) or annealing of silver films. In case of IBM, Ag films were irradiated by 400 keV Ar ions at normal incidence and at low (1×10^{16} Ar/cm^{-2}) or high (2×10^{16} Ar/cm^{-2}) ion fluence to produce the nanoparticles as reported elsewhere [6]. One

 ISBN: 978-1-61208-431-2

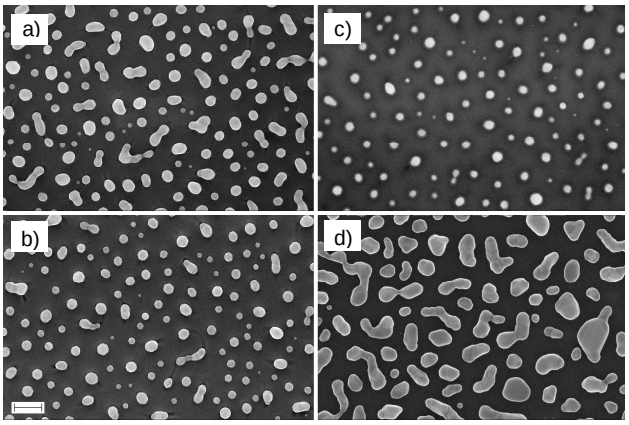

Figure 1. Plan SEM images of low (a) and high (b) dose Ar IBM samples, Xe IBM sample (c) and annealed sample (d). Scale bar is 200 nm.

sample was processed by IBM with Xe ions at dose 6×10^{15} Ar/cm^{-2}. In the case of annealing, silver films were heated at 350 ºC during 10 minutes. Annealing was done in diffusion furnace in nitrogen ambient. Further details about samples and processing can be found elsewhere [7][8]. To cover the nanoparticles with a SiO_2 layer we used a plasma enhanced chemical vapor deposition (PECVD) technique. Metal deposition and ion irradiation were perfomed at room temperature. ALD and PECVD processes were run at low temperatures 200 ºC and 170 ºC, respectively to avoid Ag oxidation. To examine the nanoparticle formation in the structures created, the images of the samples were taken with a Zeiss Supra 40 field emission scanning electron microscope. Three such images, depicting effect of IBM dose and mixing ions are shown in Figure 1(a)-(c). One more image of the sample prepared by annealing of silver film is presented in Figure 1(d). The details of nanopartile size distribution and sample surface morphology can be found elsewhere [6][9].

The optical extinction and reflection spectra were measured with a PerkinElmer Lambda 950 UV-VIS spectrometer in the range from 250 to 850 nm. Reflectance spectra at the angle of light incidence 8º were obtained by using an integrating-sphere detector incorporated in the spectrometer. Either total reflectance or diffuse reflectance only can be measured by placing spectralon plate at the specular reflectance angle or removing it, respectively.

III. Analysis of Reflection and Extinction Spectra

In this section, we study spectra of silver nanostructures on different substrates. In subsections III-A and III-B, visible parts of spectra are discussed, while the subsection III-B is devoted to UV features of the spectra.

A. Ag Nanoparticles on a Quartz Substrate

Silver nanostructures on a weekly reflecting substrate without any additional layers between nanostructures and the substrate are studied in this subsection. It simplifies spectrum analysis due to excluding from consideration interference effects. In Figure 2 (a)(b) extinction, reflection and scattering

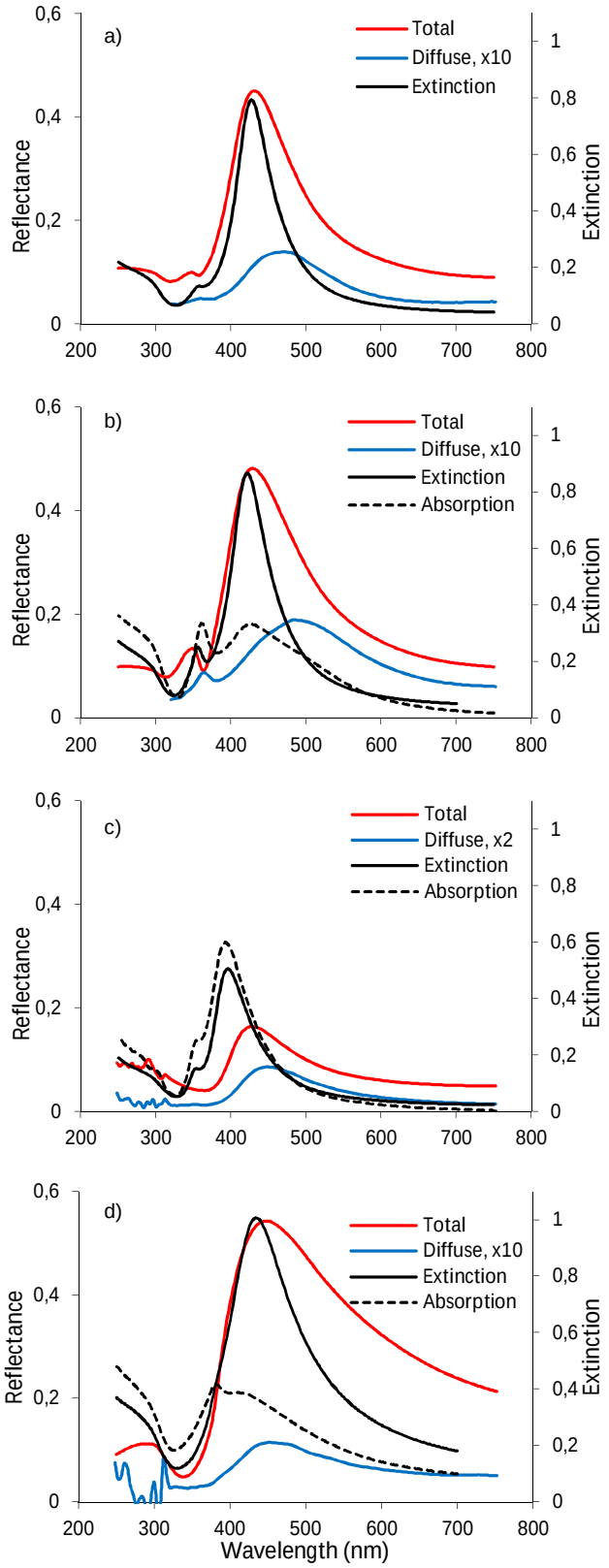

Figure 2. Spectra of low (a) and high (b) dose Ar mixed samples, RIE treated sample (c) and SiO_2 capped sample (d).

of silver nanoislands on quartz substrate are demonstrated for high and low dose of IBM, respectively. The corresponding SEM images of the samples are given in Figure 1. In the spectra, there are distinctly visible two areas: right one (wavelength more than 400 nm) with broad and intense peak in visible (VIS) range and left one (wavelength is less than 400 nm) with weak peak in ultraviolet (UV) range. Further, we call these parts as VIS and UV, respectively. The high amplitude peak is usually attributed to dipolar LSPR, whereas the low amplitude one is connected with quadrupolar LSPR [3] [9][10]. Theoretically, LSPR exhibits itself at the same wavelength in extinction and scattering [2]. However, it is valid only for isolated nanoparticles without size variation. In Figure 2 (a)(b) we observe difference in peak positions for extinction and diffuse reflection, while coinciding for extinction and total reflection peaks. Standard explanation of the observed difference is the size variation of plasmon nanoparticles. Scattering cross-section is higher for larger nanoparticles possessing lower frequency LSPR, while extinction cross-section is higher for smaller nanoparticles having LSPR at higher frequency. As a result, extinction and scattering peaks are separated. The same argument is used for explaining an increased full width at a half maximum (FWHM) of peaks in comparison with calculated ones [2]. Peak asymmetry is usually explained by shape deviation of nanoparticles from sphere to ellipsoid. It results in splitting of one LSPR in two separate resonances (redshifted and blueshifted), which can lead to observable shape of dipolar peak.

UV resonance manifestation is usually attributed to valley near 360 nm in total reflection as well as to peak at 350 nm in extinction [6][9][11] and is ascribed to quadrupolar resonance. There is also a peak at 330 nm in total reflection clearly visible in low dose sample (Figure 2 (b)). As a whole, UV features are more intense in low dose sample than in high dose one, but dipolar peak intensity is practically the same in both samples.

In Figure 2 scattering spectra are also shown. In comparison with total reflectance, for which wavelength of maximum is independent on IBM dose, difference in position of diffuse reflection peaks is 20 nm for the low and high dose samples. Intensity of scattering is 20 times less than intensity of total reflection and we can equate it with specular reflection. The samples scatter most of radiation in direction of specular reflection. It is only possible, if all radiating points, i.e., silver nanoparticles work in phase and have similar radiation patterns. If we consider our samples as diffracting gratings, then specular reflection is possible at the zero-order grating condition on the period Λ, which is expressed as [12]

$$\Lambda < \frac{\lambda}{n \sin\theta + n}, \quad (1)$$

where λ is wavelength, θ is incident angle and n is refractive index of ambient. For $\theta = 8^{o}$ and $n = 1$ the inequality (1) is simplified to $\Lambda < \lambda$. This condition is fulfilled for all wavelengths in our experiments and provides specular reflection of the arrays despite of scattering of any separate nanoparticle. Phase shift $\Delta\varphi$ appearing between incident and emitted radiation can be calculated as [1]

$$\Delta\varphi = arctan\frac{2\beta\omega}{\omega_0^2 - \omega^2}, \quad (2)$$

where β is a damping constant, ω_0 is the plasmon resonance frequency and ω is the frequency of incident wave. According to (2), $\Delta\varphi$ is changed from 0º at low frequency to 180º at high frequency and is equal 90º at the resonance wavelength. In irregular array, we can consider the most probable phase shift $\Delta\varphi_A$ of the whole array and variable phase shift $\Delta\varphi_P$ of an individual particle. If $\Delta\varphi_A$ and $\Delta\varphi_P$ are different for the same wavelength, then the particle is atypical and contributes to scattering, in the opposite case the particle takes part in specular reflection. The largest difference $\Delta\varphi_A - \Delta\varphi_P$ happens at resonance wavelength of the atypical nanoparticle and leads to highest scattering intensity of the nanoparticle. Therefore, the peak of diffuse reflection indicates wavelength of LSPR for ensemble of atypical particles, which shape and size are far away from the most probable ones. This peak is redshifted relatively specular LSPR due to larger size and asymmetrical shape of atypical particles. Therefore, diffuse reflection is more sensitive to shape and size fluctuations of nanoparticles than specular reflection. In Figure 2 (a)(b) the low dose sample has higher intensity and redshift of scattering than the high dose sample, because with increasing of IBM dose particle shape variation diminishes and particle size distribution converges to average size. As a result of analysis of Figure 2 (a)(b), we can conclude that extinction and diffuse reflection both demonstrate positions of LSPRs. However, these positions are attributed to LSPRs of different nanoparticles, they do not coincide and the difference exceeds 50 nm.

The low dose sample was additionally treated by reactive ion etching (RIE) as reported elsewhere [5][13][14]. As a result, oxide between Ag nanoislands was removed and SiO_2 pillars with a height of 50 nm were fabricated. Ag nanoparticles were left at the top of pillars. The purpose of experiment was to change the dielectric environment and to reduce possible coupling between nanoparticles. The obtained spectra of pillar sample are shown in Figure 2 (c). Additionally, in Figure 2 (b)(c) is also shown absorption $A = 1 - T - R$, where T and R are transmittance and reflectance, respectively. The dipolar extinction, absorption and scattering peaks were blueshifted on 30 - 50 nm, due to replacing SiO_2 ($\varepsilon = 2.5$) between nanoparticles by air ($\varepsilon = 1$). However, the peak of total reflection was left at the same position. Intensity of extinction and total reflection decreased 1.5 and 3 times, respectively, but intensity of absorption and scattering increased 2 and 2.5 times, respectively. The UV peak of absorption and extinction (peak and valley in reflection) was replaced by shoulder in absorption (extinction) and broad depression in reflection. Based on absorption results in VIS part (Figure 2 (b)(c)) we conclude that above mentioned deviation between absorption LSPR and reflection LSPR is attributed to different sensitivity of both methods to coupling of nanoparticles. We suppose that short wavelength dipolar LSPR (around 420 nm) visible in absorption corresponds to

 ISBN: 978-1-61208-431-2

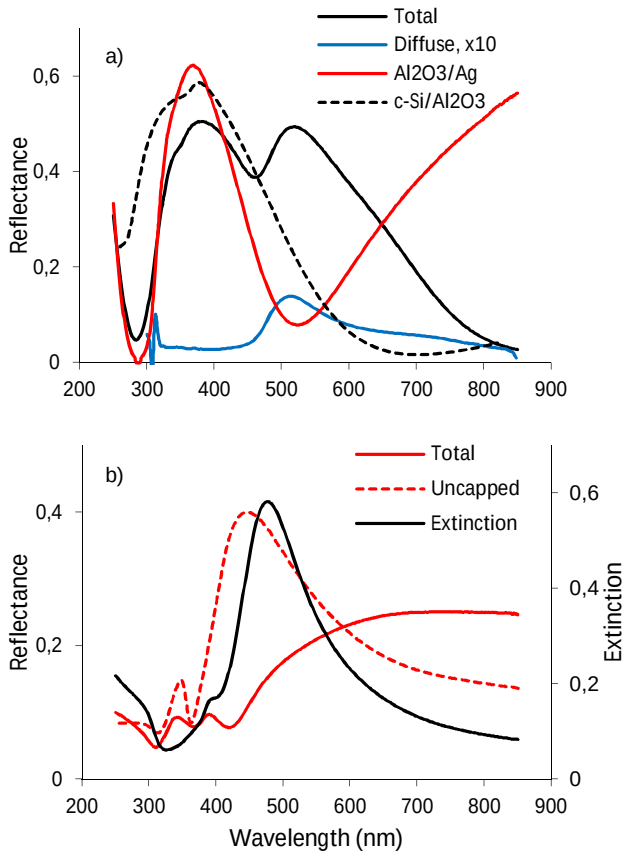

Figure 3. Spectra of Xe mixed Ag nanoparticles on 100 nm Al_2O_3 /*c*-Si (a) and of high dose Ar mixed nanoparticles on quartz, capped by 73 nm SiO_2/15 nm Ag (b).

resonance of isolated, not coupled dipoles (nanoparticles). The long wavelength LSPR (around 500 nm) visible in total reflection corresponds to coupled dipoles, where electromagnetic field is concentrated between dipoles in SiO_2. Removing of SiO_2 causes significant increase of absorption and decrease of reflection, because coupled particles transform in isolated ones. However, large nanoparticles at a small distance from each other remain coupled after RIE. They contribute in total reflection, but at longer wavelengths due to size dependence of LSPR. As a result, this redshift compensates the blueshift due to decrease of ε and peak wavelength of total reflection is not changed.

One more variation of dielectric environment was done by covering (capping) of Ag nanoparticles by oxide layer. It was realized by IBM of silver layer covered by 12 nm of SiO_2, which resulted in Ag nanoparticles embedded inside of SiO_2 matrix. Figure 2 (d) shows spectra of Ag nanoparticles capped by SiO_2. Intensity of VIS extinction is a little higher than in uncapped sample, due to higher amount of silver (capping layer prevents Ag sputtering during IBM). Intensity of total reflection increases due to stronger coupling between nanoparticles in the medium with higher ε. It is known that radiation of dipole pair (dimer) is more intensive than simple sum of isolated dipole radiations [4]. The more dimers appear after capping of nanoparticles, the higher is radiation intensity. The same effect with opposite sign decreases the total reflection of RIE processed samples (Figure 2 (c)). Coupling also makes VIS peaks much wider, due to increased extinction and reflection at long wavelengths. Scattering in capped sample is weak due to total internal reflection in SiO_2 layer. Absorption band near 400 nm is quite broad, because it is attributed to combine effect of redshifted quadrupolar resonance (390 nm in SiO_2) and dipolar LSPR.

B. Ag Nanoparticles on a Multilayer Substrate

In the subsection III-A, we demonstrated that substrate facilitates coupling between nanoparticles. It, in turn, increases intensity of radiation and results in splitting of one-peak LSPR in blueshifted (transversal) LSPR and redshifted (longitudinal) LSPR. Furthermore, multilayer substrate provides additional reflection interfaces and corresponding interference patterns in reflection. We start analysis of multilayer substrates from demonstration of phase shifting during LSPR. Figure 3 (a) shows spectra of Xe mixed Ag nanoparticles on 100 nm thick Al_2O_3 layer above *c*-Si substrate. Here is also given reflectance spectrum of 15 nm thick Ag film above Al_2O_3 before IBM. This spectrum demonstrates transparency of 15 nm thick silver film and high quality interference in Al_2O_3 optical cavity with Si and Ag mirrors. The minimum at 290 nm and maximum at 380 nm are close to theoretical interference extrema, calculated with bulk silver optical constants. After formation of nanoislands, the minimum at 530 nm is replaced by new one at 460 nm, which is quite close to wavelength of scattering peak at 510 nm, i.e., LSPR of Ag nanoparticles. When in the optical cavity one of the mirrors is replaced with plasmonic structure, the phase shift balance for extrema is [10]

$$2\Delta\varphi_{prop} + \Delta\varphi_{refl} + \Delta\varphi_{pl} = N\pi, \qquad (3)$$

where $\Delta\varphi_{prop}$ is the phase shift due to propagation of the wave through cavity, $\Delta\varphi_{refl}$ is the phase shift upon reflection at the cavity mirror, $\Delta\varphi_{pl}$ is the phase shift on plasmon structure, N is integer. Wavelength of local minimum in Figure 3 (a) is 460 nm, what corresponds $2\Delta\varphi_{prop} = 1.47\pi$ ($n_{Al2O3} = 1.69$). Additional phase shift $\Delta\varphi_{pl} = 0.53\ \pi$ provides condition for destructive interference ($\Delta\varphi_{refl} = \pi$) at 460 nm according to (3). This interference happens between light waves emitted by upper and lower lobes of dipole radiation pattern. These lobes are coherent and in phase immediately after scattering. Then, the lower wave radiated in the substrate acquires additional phase shift during propagation and reflection and interferes with upper wave. As a result, presence of optical cavity splits LSPR in two local extrema visible in total reflection. In contrast to extinction, where LSPR exhibits only one peak, the reflection spectrum demonstrates peak and valley at frequencies below and higher than resonance one. For example, in Figure 3 (a) LSPR is redshifted on 0.03π from the local minimum, because $\Delta\varphi_{pl} = 0.53\ \pi$ and $\Delta\varphi = 0.5\ \pi$ at the resonance.

To validate this suggestion for quadrupolar LSPR, the high dose Ar mixed Ag nanoparicles on quartz substrate were covered by 73 nm thick SiO_2 layer and 15 nm thick silver.

 ISBN: 978-1-61208-431-2

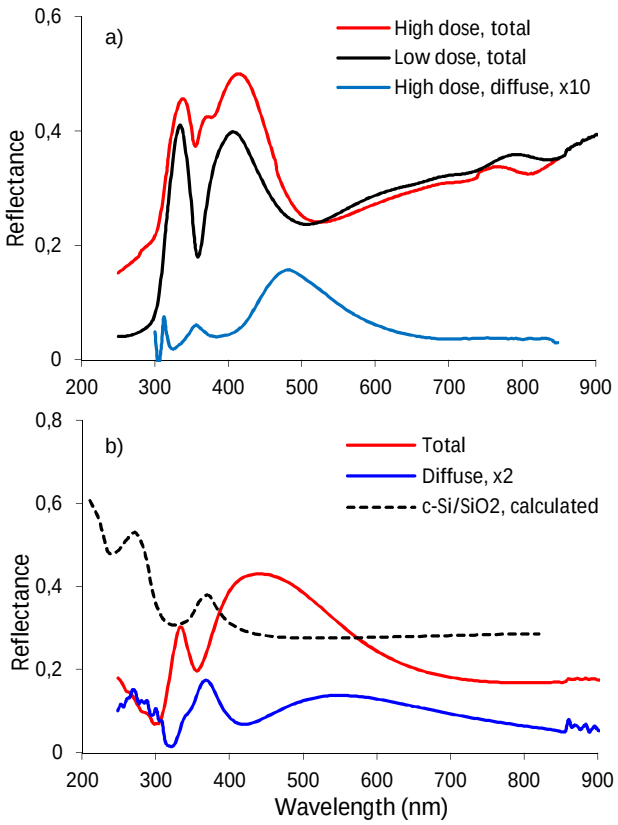

Figure 4. Spectra of Ar mixed Ag nanoparticles on 20 nm SiO_2 /*c*-Si (a) and of annealed Ag nanoparticles on 36 nm SiO_2 /*c*-Si (b).

Total reflection for uncapped nanopaticles, as well as extinction and total reflection after deposition of SiO_2/Ag are shown in Figure 3 (b). Without capping oxide the obtained reflectance spectrum is similar to spectrum in Figure 2 (b). Capping of Ag nanoparticles by SiO_2 and silver results in interference picture and reduced intensity of reflection in UV part. The minimum at 430 nm is connected with destructive interference in the capping SiO_2 layer, i.e., $2\Delta\varphi_{prop} = \pi$. According to extinction spectra (Figure 3 (b)), the quadrupolar LSPR is redshifted in SiO_2 and takes place at 390 nm. Phase shift of this LSPR $\Delta\varphi_{pl}$ transfers uprising trend in reflection after minimum at 430 nm in decreasing trend between 395 nm and 370 nm. At wavelength of local minimum 370 nm $2\Delta\varphi_{prop} = 1.15\ \pi$, $\Delta\varphi_{refl} = \pi$ at the uppermost Ag film. It means that additional phase shift 0.85 π due to LSPR will bring reflection to destructive interference. The quadrupolar LSPR is located at phase distance 0.85 π -0.5 π = 0.35 π from the minimum at 370 nm, i.e., between 370 and 395 nm.

Figure 4 (a) demonstrates total and diffuse reflection for Ar mixed Ag nanoparticles prepared on Si substrate covered by 20 nm of SiO_2. The fabrication procedure is the same as for samples on quartz substrate in Figure 2 (a)(b). The obtained spectra look similar to spectra in Figure 2 (b) in UV part. They contents the same peak 330 nm and valley 360 nm. Nevertheless, VIS parts of the spectra in Figure 2 (b) and Figure 4 (a) are different. There are two reasons for this: splitting of LSPR due to dipole coupling and reflection from

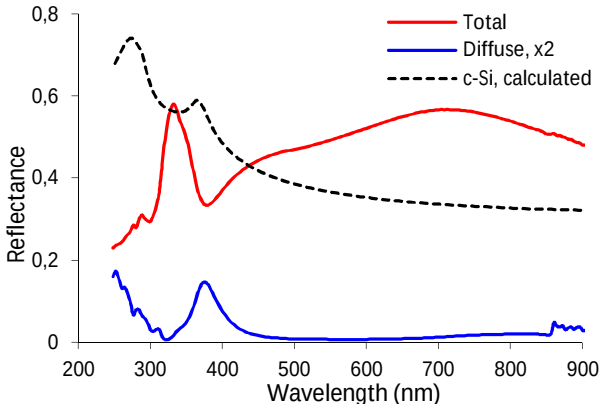

Figure 5. Spectra of annealed Ag nanoparticles on bare *c*-Si (a).

SiO_2/Si interface. According to position of the scattering peak LSPR of isolated nanoparticles happens at wavelength shorter than 480 nm. It provides rise of reflection around 400 nm. The increase of total reflection for wavelengths more than 510 nm is explained by hybridized longitudinal LSPR. The valley at 510 nm is overlapping point of coupled and isolated resonances. Phase shift increasing of isolated LSPR takes place between 410 nm and 510 nm. At the wavelength of 410 nm, the $2\Delta\varphi_{prop} = 0.29\pi$ ($n_{SiO2} = 1.47$) and $\Delta\varphi_{refl} = \pi$. Additional phase shift $\Delta\varphi_{pl} = 0.71\ \pi$ leads to peak at 410 nm. Again, LSPR in reflection can be found between local extrema, at the phase distance 0.21 π from the peak. The reflection spectrum of high dose sample demonstrates one more quadrupolar resonance at 390 nm (compare with extinction in Figure 3 (b)). It is attributed to Ag nanoparticles submerged in SiO_2 during IBM [9].

Spectra of Ag nanoparticles prepared by annealing on oxidized Si substrate (36 nm thick SiO_2) are given in Figure 4 (b). They are similar to spectra in Figure 4 (a) in UV part. The VIS part of Figure 4 (b) has a broader dipolar peak and redshifted valley as compared with similar features in Figure 4 (a). Dipole coupling happens mainly through Si substrate, due to higher ε of silicon. This means that thicker oxide decreases coupling and LSPR splitting. It can be observed as less separation of LSPR wavelengths for isolated and coupled nanoparticles. As a result, two peaks are transformed in one broad peak. The trough is redshifted, because the longitudinal LSPR is blueshifted.

Figure 5 demonstrates reflection and scattering of silver nanoparticles on bare silicon substrate. This sample was prepared by annealing. It has the same spectrum features as IBM samples on quartz (Figure 2 (b)), only UV minimum of reflection is redshifted to 380 nm. Due to higher ε dipolar coupling is very strong and broad range of split LSPRs from 450 nm to 900 nm is observed.

C. UV features of the spectra

All studied samples, exclude the 100 nm Al_2O_3/Ag and capped ones, demonstrate 330 nm peak and 360 nm trough in the UV part of reflection spectra. Moreover, in the RIE processed sample, both features were observed in as prepared nanoparticle array and disappeared after RIE (Figure 2 (c)(d)).

 ISBN: 978-1-61208-431-2

Therefore, existing of reflective surface with phase shift close to π below Ag nanoparticles is essential for obtained results. Wavelength of UV peak (330 nm) does not depend on nanostructure shape and substrate ε. The peak can be attributed to variation of reflection phase at Ag/air and Ag/substrate interfaces according with wavelength and coincides with maximum of silver refractive index n_{Ag}. Replacing air by SiO_2 (capping) or reflective surface by pillars changes reflection conditions and the mentioned UV features disappear.

Position of UV peak in absorption (360 nm) strictly coincides with the peak of diffuse reflection (Figure 2 (b), Figure 4 and Figure 5). It means that this feature is a quadrupole LSPR [10]. However, its position weakly depends on dielectric environment and for Si substrate with high ε valley is moved only to 375 nm (Figure 5). At the same time, quadrupolar LSPR of submerged in oxide Ag particles is shifted to 390 nm (Figure 4 (a)). Additionally, extinction coefficient of silver has minimum and reflection has maximum at the same wavelength 360 nm (see calculated spectra at Figure 4 (b) and Figure 5), which in turn, facilitates destructive interference. We believe that all these factors contribute in stable position of 360 nm valley.

IV. CONCLUSIONS

We have demonstrated that peaks and valleys in reflectance spectrum of nanoparticles on multilayer substrates do not correspond directly to plasmon resonances. However, it is possible to identify position of LSPR with accuracy of FWHM of resonance band. This position is situated between two local extrema of reflectance spectrum, corresponding phase shift variation during LSPR. The spectrum features in UV range may be attributed either to quadrupolar resonance or to variation of reflection phase. In the first case, the valley position depends on dielectric environment and geometry of plasmonic structures. In the second case, the peak is fixed at 330 nm and observed only in nanostructures having silver/air interface and formed on smooth reflecting surface. The obtained results can be used in analysis and design of plasmonic nanostructures on opaque substrates.

ACKNOWLEDGMENT

This research was undertaken at the Micronova Nanofabrication Centre, supported by Aalto University.

REFERENCES

[1] R. Ameling et al., “Cavity-enhanced localized plasmon resonance sensing”, Appl. Phys. Lett., v.97, 2010, pp. 253116-1 – 253116-3.

[2] E. C. Le Ru and P. G. Etchegoin, “Principles of Surface-Enhanced Raman Spectroscopy and Related Plasmonic Effects”, Elsevier, 2008, 688 p.

[3] S.Pillai, K. R. Catchpole, T. Trupke, and M.A. Green, “Surface plasmon enhanced silicon solar cells”, J. Appl. Phys., v.101, 2007, pp. 093105-1 - 093105-8.

[4] P. Biagioni, J.-S. Huang, and B. Hecht, “Nanoantennas for visible and infrared radiation”, Rep. Prog. Phys., v.75, 2012, pp. 024402-1 - 024402-40.

[5] 5. A. Shevchenko, V. Ovchinnikov, and A. Shevchenko “Large-area nanostructured substrates for surface enhanced Raman spectroscopy”, Appl. Phys. Lett., v. 100 (17), 2012, pp. 171913-1 - 171913-4.

[6] V. Ovchinnikov and A. Priimagi, “Anisotropic Plasmon Resonance of Surface Metallic Nanostructures Prepared by Ion Beam Mixing”, Proceedings of the First International Conference on Quantum, Nano and Micro Technologies (ICQNM'07), 2-6 January 2007, Guadeloupe, French Caribbean, IEEE XPlore Digital Library, ISBN: 978-1-4244-3131-1, icqnm, 2007, pp. 3-8.

[7] V. Ovchinnikov, “Analysis of Furnace Operational Parameters for Controllable Annealing of Thin Films”, Proceedings of the Eighth International Conference on Quantum, Nano/Bio, and Micro Technologies (ICQNM 2014), November 16 - 20, 2014, Lisbon, Portugal, ThinkMind Digital Library (ISBN: 978-1-61208-380-3), 2014, pp. 32-37.

[8] V. Ovchinnikov, “Effect of Thermal Radiation during Annealing on Self-organization of Thin Silver Films”, Proceedings of the Seventh International Conference on Quantum, Nano and Micro Technologies (ICQNM 2013), August 25-31, 2013, Barcelona, Spain, ThinkMind Digital Library (ISBN: 978-1-61208-303-2), 2013, pp. 1-6.

[9] V. Ovchinnikov, “Formation and Characterization of Surface Metal Nanostructures with Tunable Optical Properties”, Microelectronics Journal, v.39(3-4), 2008, pp. 664-668.

[10] E. Thouti, N. Chander, V. Dutta, and V. K. Komarala, “Optical properties of Ag nanoparticle layers deposited on silicon substrates”, J. Opt., v.15, 2013, 035005-1 - 035005-7.

[11] V. Ovchinnikov and A. Shevchenko, “Surface Plasmon Resonances in Diffusive Reflection Spectra of Multilayered Silver Nanocomposite Films”, Proceedings of the Second International Conference on Quantum, Nano and Micro Technologies (ICQNM 2008), 10-15 February 2008, Sainte Luce, Martinique, IEEE Computer Society Digital Library, ISBN: 978-1-4244-4228-7, icqnm, 2008, pp. 40-44.

[12] Tian Sang et al., “Systematic study of the mirror effect in a poly-Si subwavelength periodic membrane”. J. Opt. Soc. Am. A, 26 (3), 2009, pp. 559-565.

[13] V Ovchinnikov, A Malinin, S Novikov, and C Tuovinen, “Silicon nanopillars formed by reactive ion etching using a self-organized gold mask”, Physica Scripta (T79), 1999, pp. 263-265.

[14] A. Shevchenko and V. Ovchinnikov, “Magnetic Excitations in Silver Nanocrescents at Visible and Ultraviolet Frequencies”, Plasmonics, 4(2), 2009, pp. 121-126.

 ISBN: 978-1-61208-431-2